CT Baggage Image Enhancement Using a Combination of Alpha-Weighted Mean Separation and Histogram Equalization

Yicong Zhou*[a], Karen Panetta[a], Sos Agaian[b]

[a]Department of Electrical and Computer Engineering, Tufts University, Medford, MA USA 02155;
[b]Department of Electrical and Computer Engineering, University of Texas at San Antonio, San Antonio, TX USA 78249

ABSTRACT

Baggage scanning systems are used for detecting the presence of explosives and other prohibited items in baggage at security checkpoints in airports. However, the CT baggage images contain projection noise and are of low resolution. This paper introduces a new enhancement algorithm combining alpha-weighted mean separation and histogram equalization to enhance the CT baggage images while removing the background projection noise. A new enhancement measure is introduced for quantitative assessment of image enhancement. Simulations and a comparative analysis are given to demonstrate the new algorithm's performance.

Keywords: CT baggage image, image enhancement, alpha-weight mean separation, histogram equalization

1. INTRODUCTION

Security systems in airports use computerized tomography (CT) scanning systems to scan and screen packages and luggage for detecting the presence of explosives and other prohibited items in baggage before loading the baggage onto a commercial aircraft [1, 2]. The systems expose the baggage to X-rays and measure the amount of radiation absorbed by the baggage. The baggage CT image is then generated from these X-ray projection densities. These images suffer from projection noise and therefore have a low resolution, especially for small objects/regions and fine details in images. Image enhancement is an effective and powerful tool to improve the visual quality of images by increasing the image's global or local contrast between regions or objects and their background surroundings, without changing system hardware.

Many enhancement techniques have been recently employed to improve the contrast of images. Histogram equalization (HE) is a well-known technique for image enhancement due to its simplicity and effectiveness [3]. However, it may significantly change the brightness of an input image and cause visually undesirable artifacts [4]. To overcome this problem, Bi-histogram equalization was proposed , combining HE with a mean-separation technique [5]. This enhancement method strives to preserve the mean brightness of original image. Many HE-based algorithms have been developed based on image decomposition such as minimum mean brightness error bi-histogram equalization [4], recursive mean-separate histogram equalization [6], dualistic sub-image histogram equalization [7], and recursively separated and weighted histogram equalization [8].

After analyzing the characteristics of the CT baggage images in this paper, we introduce a new algorithm for enhancing CT baggage images by integrating histogram equalization with alpha-weighted mean separation for airport security applications. The new algorithm contains two processes, namely noise removal and object image enhancement. A new enhancement measure, called the second-derivative-like measure of enhancement (SDME), is also introduced to quantitatively assess the enhancement performance of the presented algorithm.

The rest of the paper is organized as followed. Section 2 analyzes the CT baggage images and introduces an image denoising method using the weighted mean separation. Section 3 introduces the new algorithm for enhancing the CT baggage images. Section 4 introduces a new enhancement measure. Section 5 introduces a training method to obtain the optimized parameters. Section 6 analyzes and compares the enhancement results. Section 7 draws a conclusion.

* yzhou0a@ece.tufts.edu ;   phone 1-617-627-5183; fax 1-617-627-3220

2. CT BAGGAGE IMAGE ANALYSIS AND DENOISING

In this section, we analyze the characteristics of CT baggage images. An image separation method is then introduced, using the alpha-weighted mean as a threshold for removing the background noise from the CT baggage images.

2.1 CT Baggage Image Analysis

The pixel values of the CT images in baggage scanning systems are represented by 16 bits. In general, only the object skeletons with high intensity values are visually recognizable, while other regions are dark as shown in Fig. 1. The bottom row in Fig. 1 plots the pixel intensity distribution of the CT baggage images in the column direction. The pixels with high intensity values are concentrated in the object regions in the image. The non-object regions in images are very dark in which the pixel values are very small but not zeros. This observation shows that there is a lot of background noise in the CT image. This can be verified by the results shown in Fig. 2.
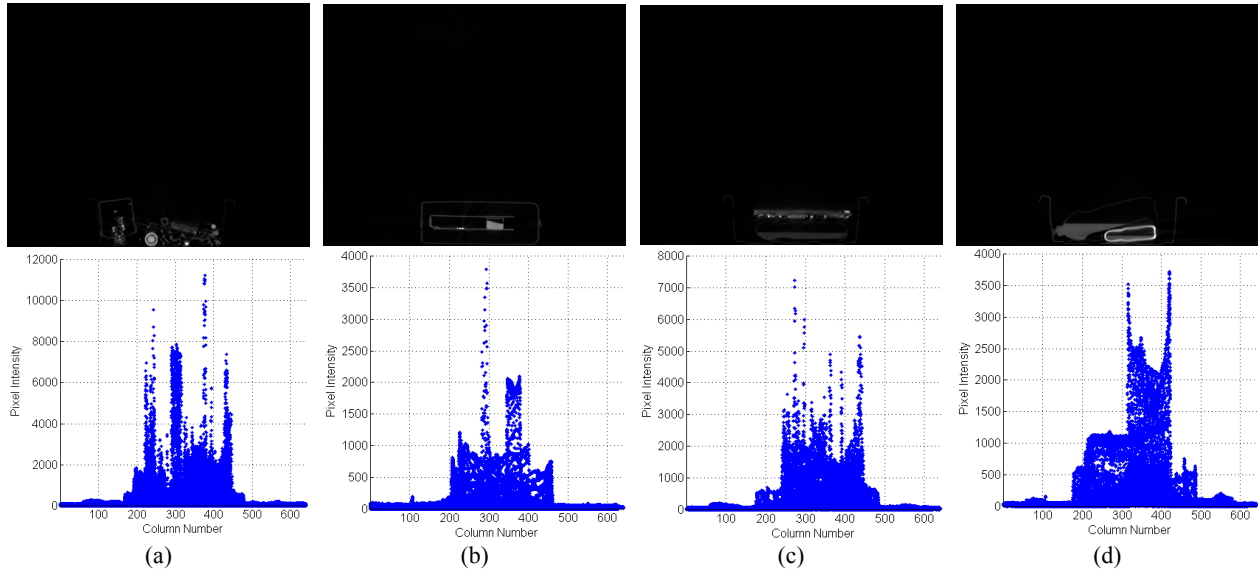

Fig. 1. CT baggage images and the pixel intensity distribution in the column direction. The top row shows original images. The bottom row shows the pixel intensity distribution in the column direction. This demonstrates that pixel intensity values are very high in the object regions and extremely low in the dark regions.
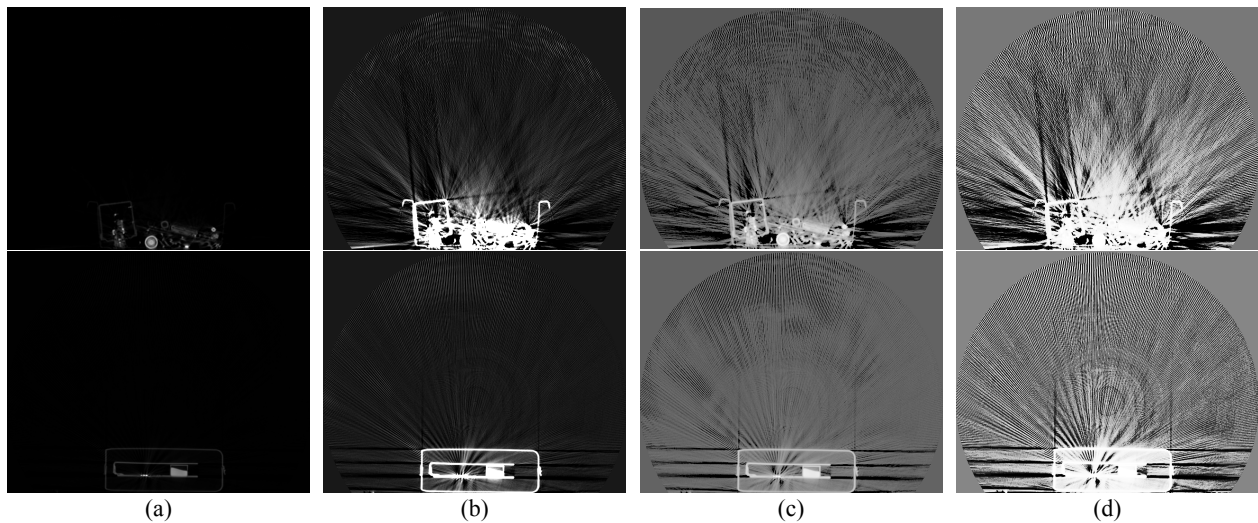

Fig. 2. CT baggage images are processed by different nonlinear operations. (a) Original images; (b) uint8; (c) logarithmic operation; (d) Histogram Equalization. This demonstrates that the CT images are in presence of projection noise

In Fig. 2, the CT baggage images are processed by three different nonlinear processes, namely the uint8 format operation, the logarithmic operation and histogram equalization. The unit8 format operation converts the data values to their nearest integers and sets data values to 255 for data values great to 255 and to zero if data value is less than zero. The logarithmic operation converts data to its natural log value. Histogram equalization is a simple nonlinear transformation used for image enhancement. The results in Fig. 2 show that the background noise becomes visible after these nonlinear processes. Since the image enhancement is also a nonlinear process, the enhancement of a CT baggage image requires a preprocess to remove the background noise.

2.2 CT Baggage Image Denoising

Since the intensity values of the background noise in CT baggage images are very small as shown in the bottom row in Fig. 1, the background noise could be separated from the CT baggage images using a thresholding technique. In this paper, we use an alpha-weighted mean value as the threshold. This is called the alpha-weighted mean separation.
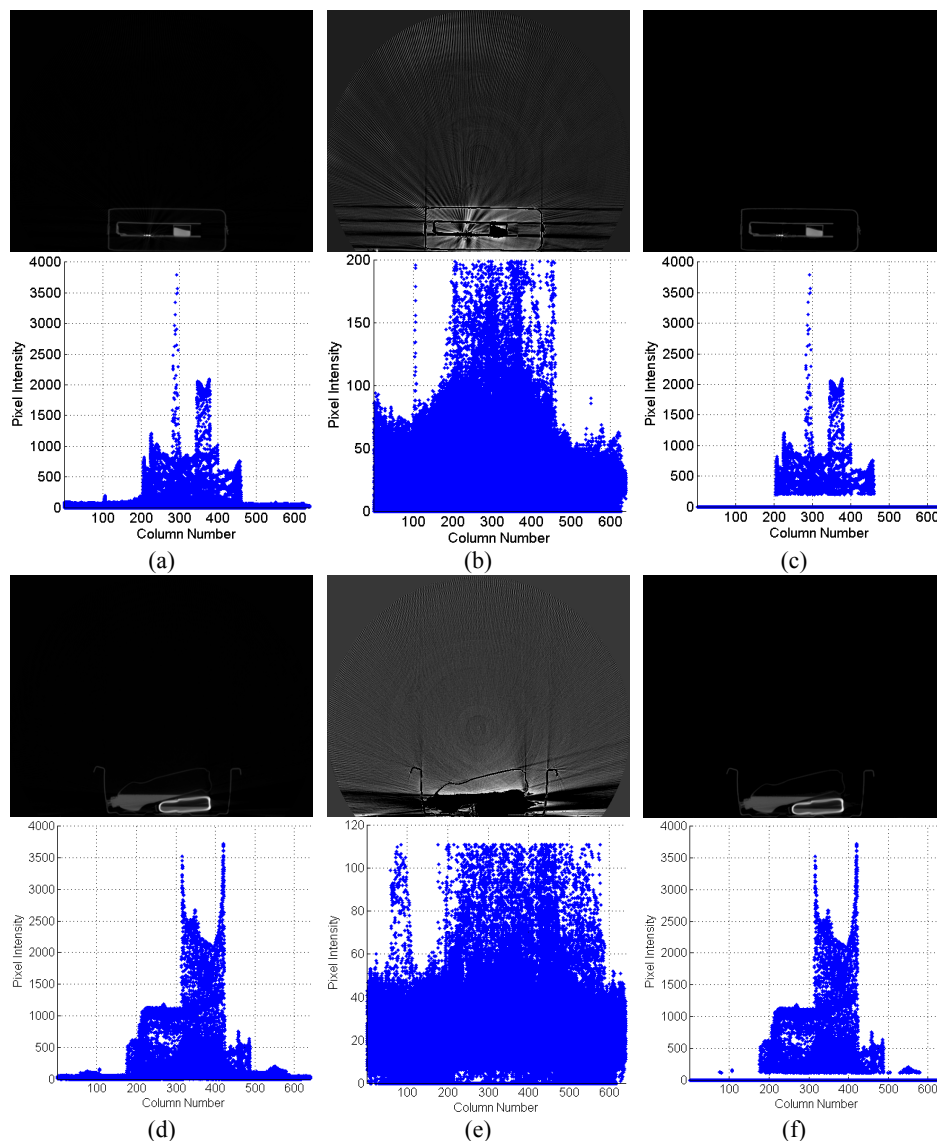

Fig. 3. Alpha-weighted mean separation of the CT baggage images. (a)-(f): the top row show the original CT baggage images and their sub-images; the second row shows their pixel intensity distributions in the column direction. (a)&(d) The original images; (b)&(e) The sub-images with pixel values less than the threshold; (c)&(f) The sub-images with pixel values greater than the threshold.

For an input image, $I(m,n)$, the separation process separates the input image into two sub-images, $I_U(m,n)$ and $I_L(m,n)$. One sub-image, $I_L(m,n)$, contains all pixels with the value lower than the threshold. The other sub-image, $I_U(m,n)$, contains the pixels with the value greater than the threshold. The maximum, mean and minimum value of the input image are I_{max}, I_{mean}, and I_{min} respectively, the alpha-weighted mean separation is defined by

$$\begin{cases} I_U(m,n) = I(m,n) & \text{for } I(m,n) \geq \alpha I_{mean} \\ I_L(m,n) = I(m,n) & \text{for } I(m,n) < \alpha I_{mean} \end{cases} \tag{1}$$

where αI_{mean} is the threshold value, and $I_{min} \leq \alpha I_{mean} \leq I_{max}$.

Fig. 3 shows two examples of the alpha-weighted mean separation of the CT baggage images. The sub-images with pixel values below the threshold contain most of background noise. The object is located in the sub-image with pixels values equal or above the threshold. These are verified by their pixel intensity distributions in the column direction.

3. NEW ENHANCEMENT ALGORITHM

Based on the image analysis and separation in Section 2, we should remove the background noise in the CT baggage images before performing an enhancement process. CT baggage images contain only the skeletons of the scanned objects. Since histogram equalization has the capability of improving the image contrast while keeping the image data range unchanged, we use this advantage for CT image enhancement. In this section, we introduce a new CT baggage image enhancement algorithm by combining the alpha-weighted mean separation with the histogram equalization techniques.

The new algorithm shown in Fig. 4 is called the alpha-weighted mean separation based histogram equalization (AWMSHE).
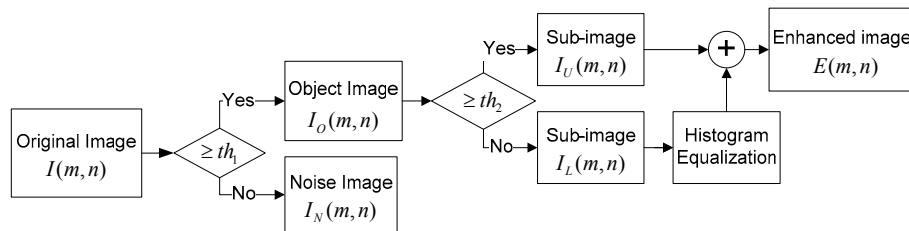

Fig. 4. Block diagram of the enhancement algorithm for the CT baggage images

The AWMSHE consists of two main processes: noise removal and object image enhancement. First, the algorithm obtains the object image by removing background noise from the original CT baggage image using the alpha-weighted mean separation as defined by,

$$\begin{cases} I_O(m,n) = I(m,n) & \text{for } I(m,n) \geq th_1 \\ I_N(m,n) = I(m,n) & \text{for } I(m,n) < th_1 \end{cases} \tag{2}$$

where $I_O(m,n)$ and $I_N(m,n)$ are the object image and the background noise image, respectively, the threshold $th_1 = \alpha_1 I_{mean}$, and I_{mean} is the mean value of the original CT baggage image.

Second, the object image is separated into two sub-images, the upper sub-image, $I_U(m,n)$, which contains the pixels with the intensity values equal or greater than the threshold th_2, and the lower sub-image, $I_L(m,n)$, which consists of the pixels with the intensity values less than the threshold th_2. This separation is defined by,

$$\begin{cases} I_U(m,n) = I_O(m,n) & \text{for } I_O(m,n) \geq th_2 \\ I_L(m,n) = I_O(m,n) & \text{for } I_O(m,n) < th_2 \end{cases} \tag{3}$$

where the threshold $th_2 = \alpha_2 I_{O\_mean}$, and I_{O_mean} is the mean value of the object image $I_O(m,n)$.

The upper sub-image includes all the bright regions in the original CT image. This sub-image has a large data range despite the fact that there are a small number of pixels with adequately high intensity values. The lower sub-image, on the other hand, contains most of the informative pixels which have lower intensity values and need to be improved. These are the reasons why the CT images are generally very dark but have a broad data range. Since histogram equalization can significantly improve the image contrast without changing the image data range, it is used to enhance the lower sub-image. The pixel intensity of the upper image could be simply clipped to the maximum value of the lower image in such a way that we can compress the data range of the images without generating additional artifacts.

Let $\{X_0, X_1, ..., X_{p-1}\}$, $X_0 < X_1 < ... < X_{p-1}$, denote all nonzero discrete gray levels in the lower image $I_L(m,n)$. For a given pixel value $I_L(m,n) = X_k$, $k = 0,1,...p-1$, then its cumulative density function is,

$$C_{I_L(m,n)} = \sum_{i=0}^{k} \frac{q_k}{q} \tag{4}$$

where q_k is the number of times that the gray level X_k appears in the lower image $I_L(m,n)$ and q is the total number of the nonzero pixels in the lower image $I_L(m,n)$.

The final enhanced image can be obtained by

$$E(m,n) = E_U(m,n) + E_L(m,n) \tag{5}$$

where,

$$\begin{cases} E_U(m,n) = X_{p-1} & \text{for } I_U(m,n) \neq 0 \\ E_L(m,n) = X_0 + (X_{p-1} - X_0)C_{I_L(m,n)} \end{cases}$$

where X_0 and X_{p-1} are the minimum and maximum values in the image $I_L(m,n)$.

Note that the enhancement process in the presented AWMSHE algorithm reverts to the traditional histogram equalization when $th_2 = I_{max}$. In this case, the lower sub-image is equal to the object image, namely $I_L(m,n) = I_O(m,n)$; the upper sub-image is zero, i.e. $I_U(m,n) = 0$.

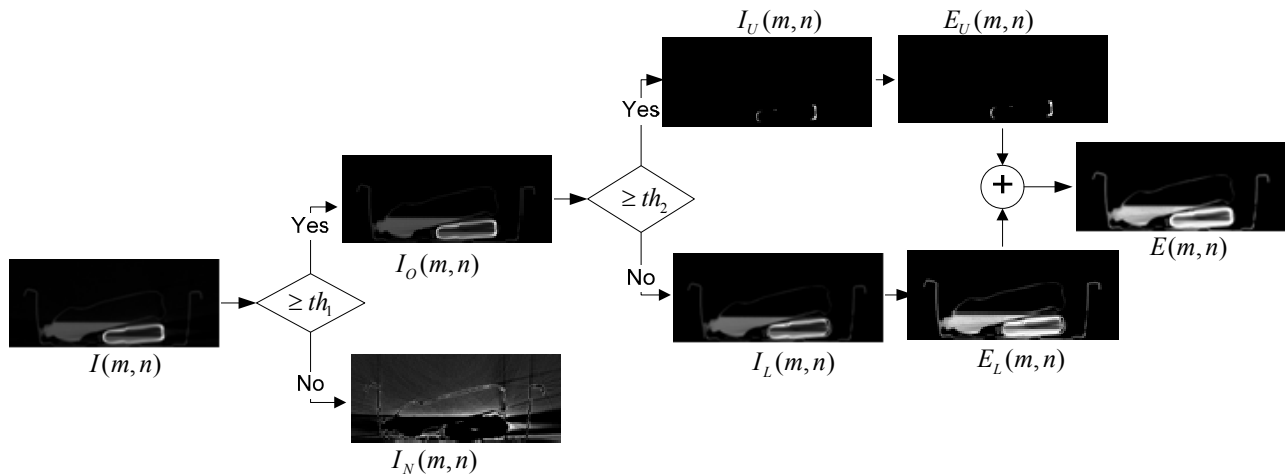Fig. 5 gives an example to show how the image changes in each process in the presented algorithm.

Fig. 5. Image changes in each step of the presented AWMSHE algorithm.

4. NEW ENHANCEMENT MEASURE

In general, an image enhancement algorithm is designed to improve image contrast. Therefore, the enhancement measure is based on contrast measure. To quantitatively assess the enhancement performance of the presented new algorithm, we introduce a new enhancement measure using the concept of the second derivative. The measure is called the second-derivative-like measure of enhancement (SDME) which is defined by,

$$SDME = -\frac{1}{k_1 k_2}\sum_{l=1}^{k_1}\sum_{k=1}^{k_2} 20\ln\left|\frac{I_{\max;k,l} - 2I_{mean;k,l} + I_{\min;k,l}}{I_{\max;k,l} + 2I_{mean;k,l} + I_{\min;k,l}}\right| \tag{6}$$

where an image is divided into $k_1 \times k_2$ blocks. $I_{\max;k,l}, I_{\min;k,l}$ and $I_{mean;k,l}$ are the maximum, minimum and mean values of the pixels in each block separately.

5. TRAIN PARAMETERS

There are two parameters in the presented AWMSHE algorithm: α_1 for noise removal and α_2 for image enhancement. In this section, we address how the parameters affect the enhanced results and the methods to select the parameters.
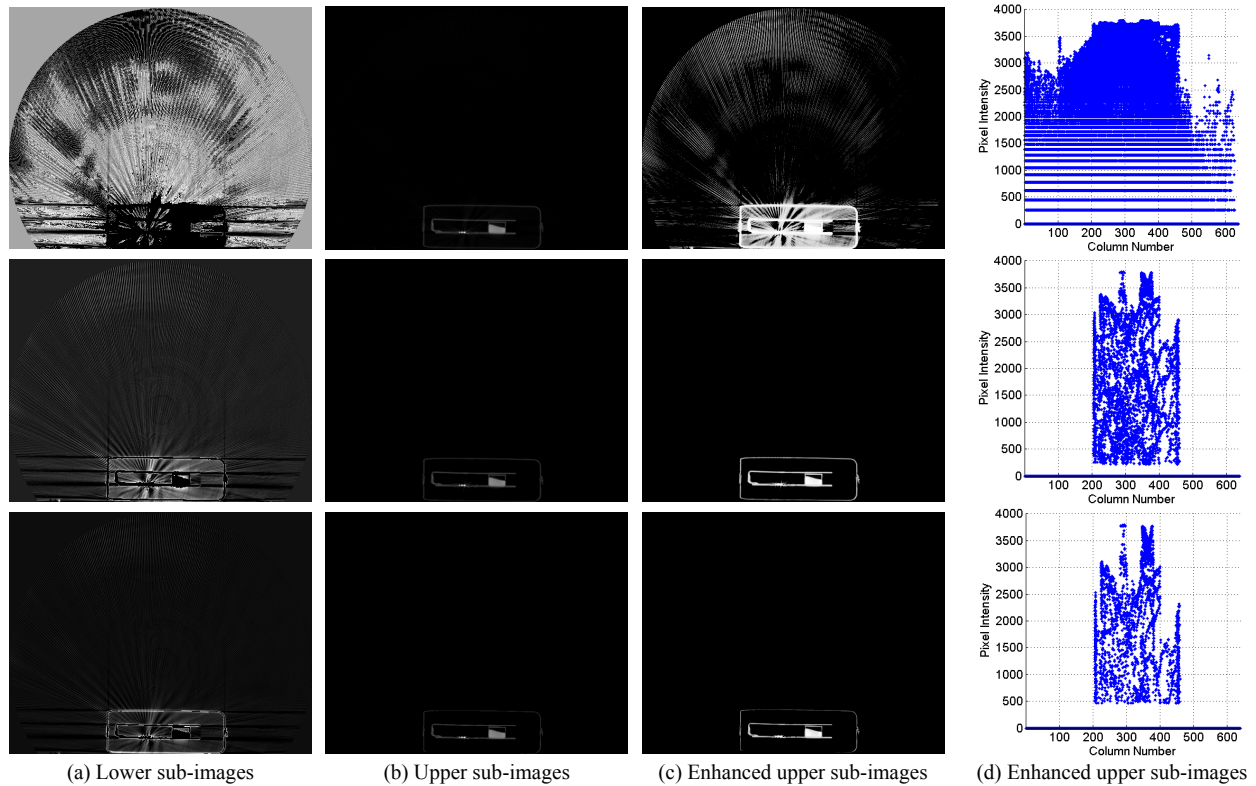

| (a) Lower sub-images | (b) Upper sub-images | (c) Enhanced upper sub-images | (d) Enhanced upper sub-images |

Fig. 6. CT baggage image separation using different alpha values. Top row: α=1; Middle row: α=5.3; Bottom row: α=12. (a) The lower sub-images, namely the noise images; (b) the upper sub-images, namely the object images; (c) the enhanced upper sub-images; (d) the pixel intensity distribution of the enhanced upper images in the column direction.

First, we train the parameter α_1 for the noise removal process. Different α_1 values are used for image separation to subtract the background noise from the original CT images. We then enhance the object images using the traditional histogram equalization which is a special case of the presented AWMSHE algorithm for $th_2 = I_{\max}$. A training example is shown in Fig. 6. If α_1 is very low, there is some background noise presented in the enhanced images as in the case shown in the top row. The background noise can be completely removed when an appropriate α_1 value is used as shown in the

middle row. However, some object information is lost if the α_1 value is very high as in the case shown in the bottom row in Fig. 6. Therefore, the α_1 value of the case in the middle row in Fig. 6 is close to the best result, which keeps the object information while removing the background noise. This observation can be verified by the pixel intensity distributions in Fig. 6(d).

For a given α_1 for the noise removal process, we then optimize the parameter α_2 for the image enhancement process. Based on the simulation results in Fig. 6, we select the same CT baggage image and α_1=5.3 for the noise removal process. Different α_2 values are applied for object image enhancement. The SDME is used to measure the enhanced images. The measure results are plotted in Fig. 7. Fig. 8 shows several enhanced images using the alpha values selected from Fig. 7. The visual quality of the original image is significantly improved. This can also be demonstrated by the SDME measure results in Fig. 8.
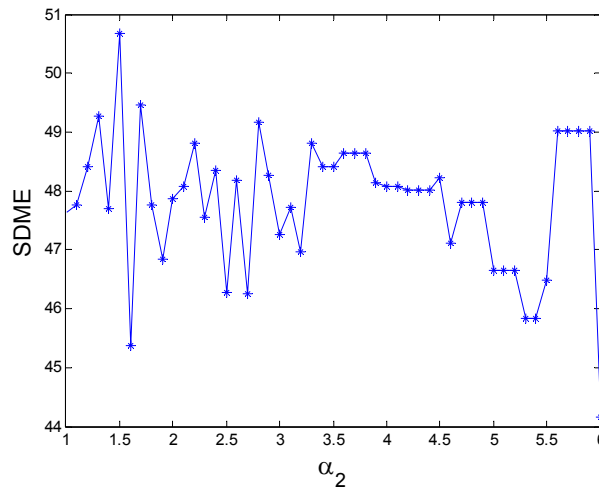

Fig. 7. SDME measure results for object image enhancement using different α_2 values.

(a) Original object image
SDME=44.3289

(b) α_2=1.6
SDME=45.37

(c) α_2=2.4
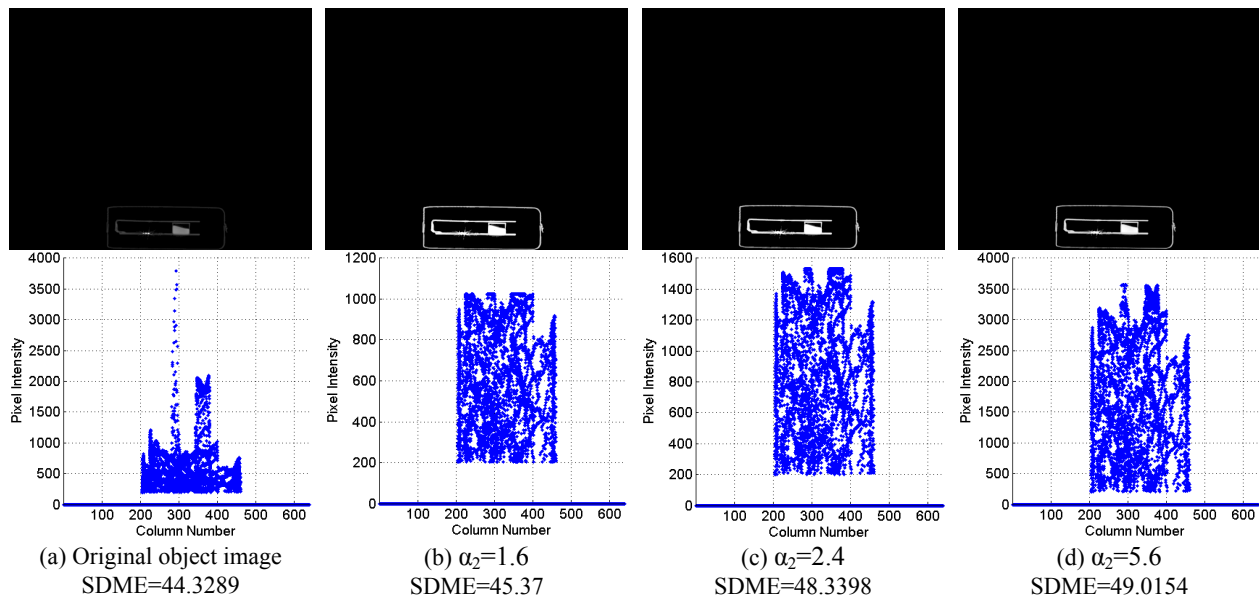SDME=48.3398

(d) α_2=5.6
SDME=49.0154

Fig. 8. Object image enhancement using different alpha values selected from Fig. 7. (a) shows the original object image obtained by the noise removal process, α_1=5.3; (b)-(d) shows the enhanced object images using different α_2 values.

6. SIMULATION RESULTS

In this section, we provide several simulation and measure results to show the AWMSHE's enhancement performance. The new algorithm is also compared with other two existing enhancement methods for the CT baggage image enhancement.

6.1 CT Baggage Image Enhancement

Fig. 9 shows the enhanced results of four CT baggage images. The images are enhanced by the presented AWMSHE individually. The original images and enhanced images are measured by the presented SDME measure. The measure results are shown in Fig. 9. To clearly show the visual improvement of the enhanced images and the original images, Fig. 10 crops the object images from the original and enhanced images in Fig. 9. The results show that the presented AWMSHE significantly improves the visual quality of the CT baggage images. The SDME measure results in Fig. 9 verify this improvement.

SDME=30.7675   SDME=33.9308   SDME=37.6769   SDME=38.002

(a) SDME=43.3394   (b) SDME=46.6898   (c) SDME=48.9462   (d) SDME=46.0667
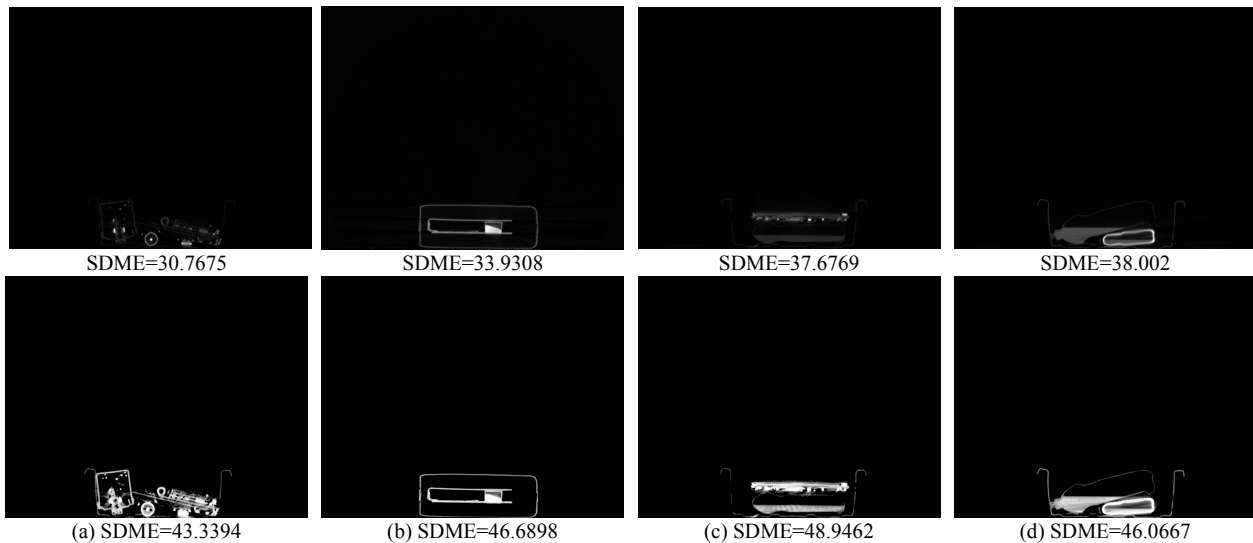
Fig. 9. CT baggage image enhanced by the presented AWMSHE algorithm. The top row shows original images. The bottom row shows the enhanced images. (a) The slice image from The volume image #1; (b) The slice image from The volume image #2; (c) The slice image from The volume image #3; (d) The slice image from The volume image #4.

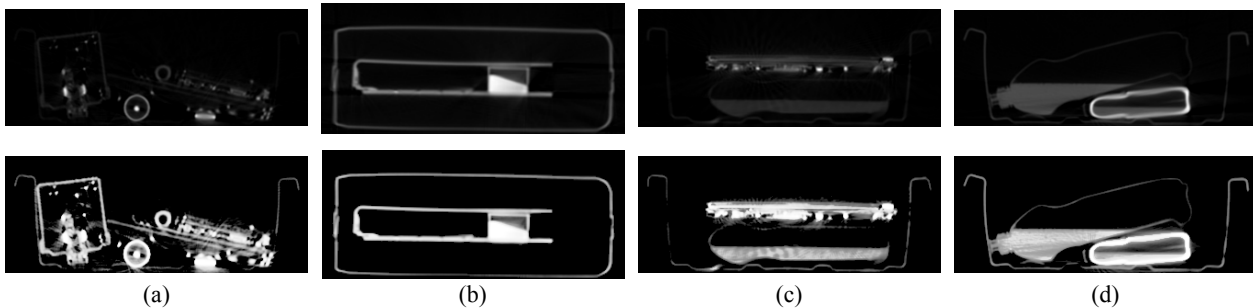(a)   (b)   (c)   (d)

Fig. 10. The regions cropped from the CT baggage images in Fig. 9. The top row shows the regions cropped from the original images. The bottom row shows the regions cropped from the enhanced images. (a) The object region cropped from the slice images in Fig 9(a); (b) The object region cropped from the slice images in Fig 9(b); (c) The object region cropped from the slice images in Fig 9(c); (d) The object region cropped from the slice images in Fig 9(d).

6.2 3D Visualization

To show the performance of the presented AWMSHE algorithm for CT baggage image enhancement, several 3D views of the object images are presented in this section. The object volume images are cropped from a CT baggage volume images to minimize background noise. Fig. 11-14 shows the 3D views of the original and enhanced object images. The top row contains the 3D views of the original object images from the top, bottom, front side and back side. The bottom

row is the 3D view of the enhanced object images from corresponding side. The visual quality of the object images is significantly improved. This demonstrates the excellent enhancement performance of the presented AWMSHE shows in CT baggage image enhancement.

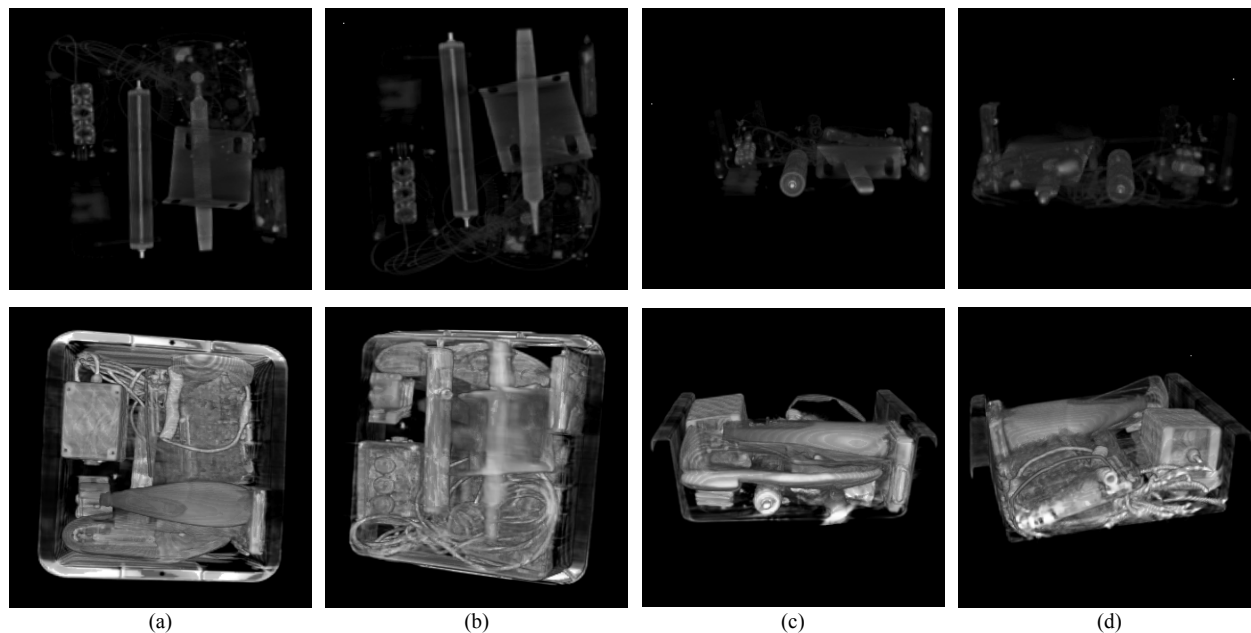| (a) | (b) | (c) | (d) |

Fig. 11. 3D visualization of the object volume image #1. Top row shows the 3D views of the original volume image; the bottom row shows the 3D views of the volume image enhanced by the presented AWMSHE algorithm. (a) Top view of the entire volume image; (b) Bottom view of the entire volume image; (c) Front side view of the slice images #31-280; (d) Back side view of the slice images #31-280.
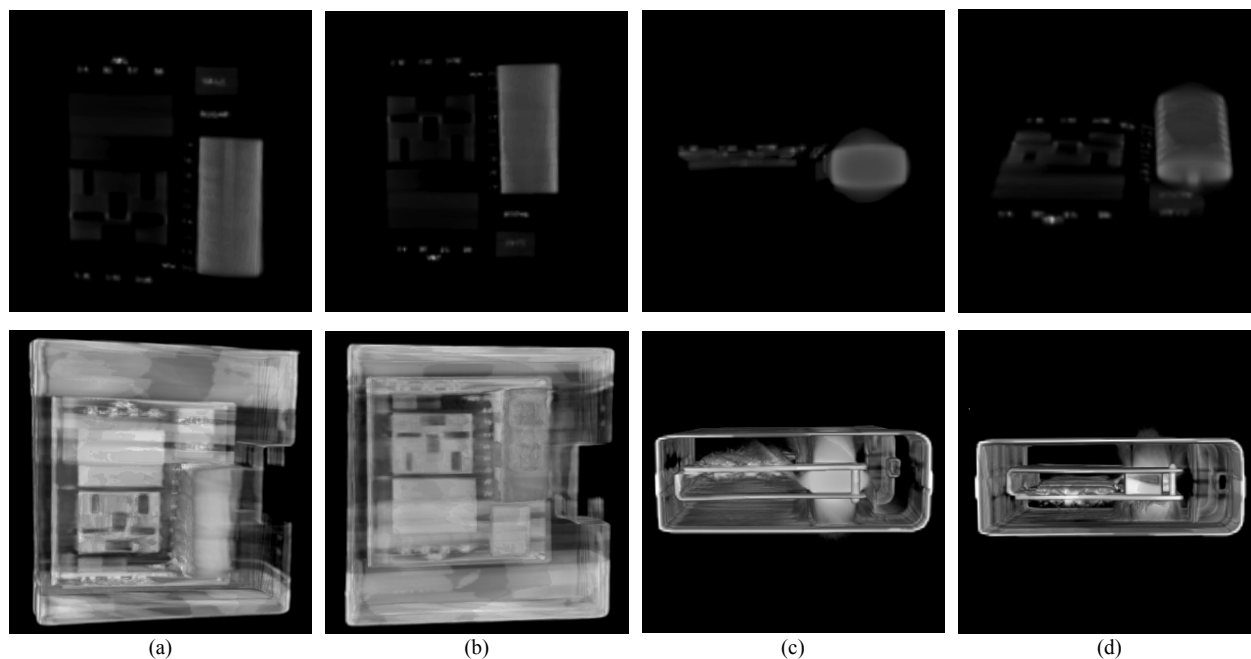

| (a) | (b) | (c) | (d) |

Fig. 12. 3D visualization of the object volume image #2. Top row shows the 3D views of the original volume image; the bottom row shows the 3D views of the volume image enhanced by the presented AWMSHE algorithm. (a) Top view of the entire volume image; (b) Bottom view of the entire volume image; (c) Front side view of the slice images #21-250; (d) Back side view of the slice images #21-250.
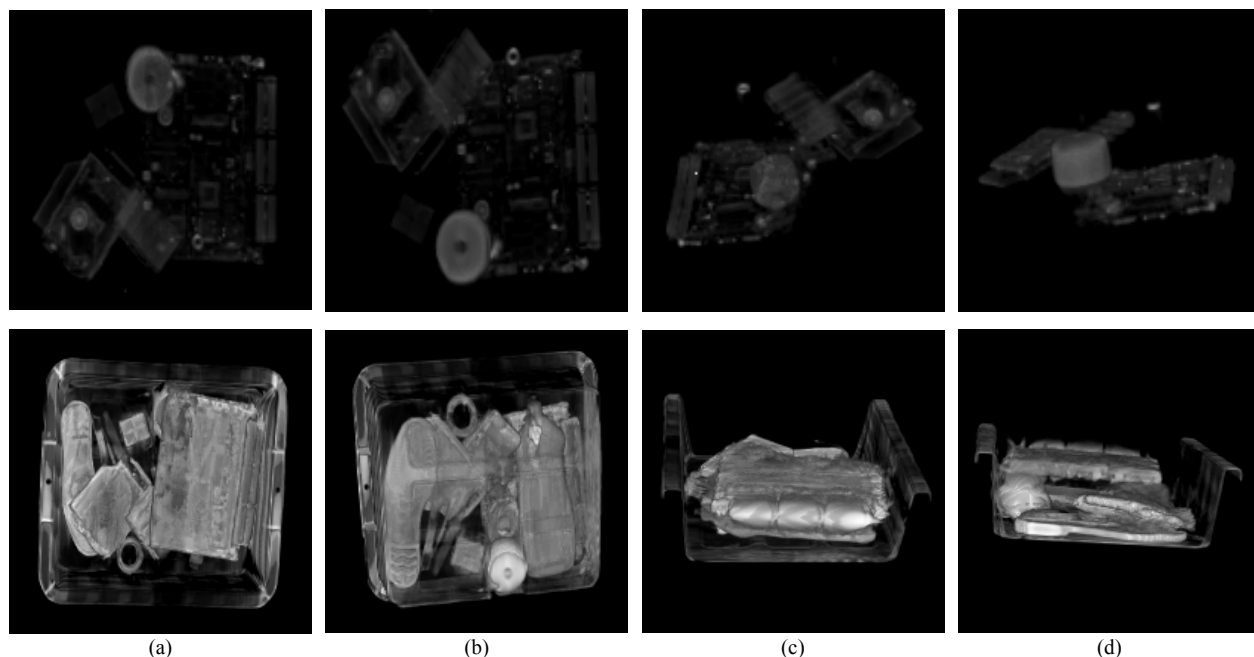
Fig. 13. 3D visualization of the object volume image #3. Top row shows the 3D views of the original volume image; the bottom row shows the 3D views of the volume image enhanced by the presented AWMSHE algorithm. (a) Top view of the entire volume image; (b) Bottom view of the entire volume image; (c) Front side view of the slice images #34-293; (d) Back side view of the slice images #34-293.
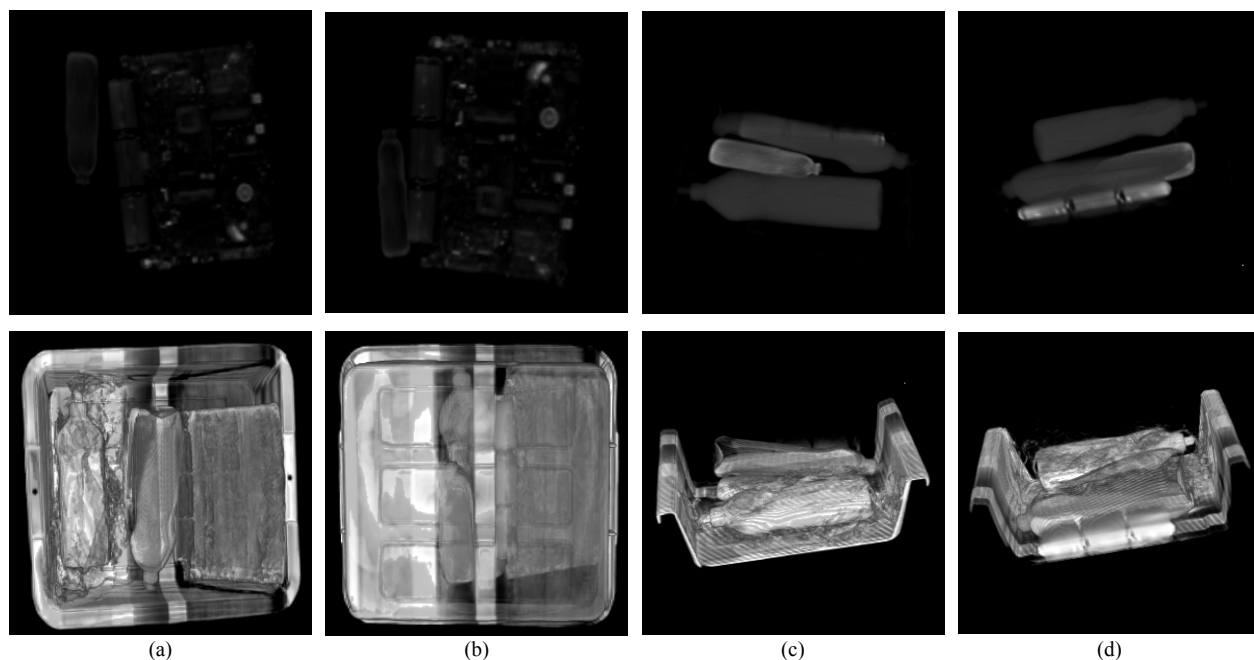

Fig. 14. 3D visualization of the object volume image #4. Top row shows the 3D views of the original volume image; the bottom row shows the 3D views of the volume image enhanced by the presented AWMSHE algorithm. (a) Top view of the entire volume image; (b) Bottom view of the entire volume image; (c) Front side view of the slice images #131-290; (d) Back side view of the slice images #131-290.

6.3 Enhancement Comparison

To show the enhancement performance of the presented AWMSHE algorithm, it is compared with two other existing enhancement methods, the alpha-weighted quadratic filter (AWQF) [9] and bi-histogram equalization (BIHE) [5]. Fig. 15 and Fig 16 give the enhancement results of two images. The enhanced images and cropped regions show that the images enhanced by the presented AWMSHE have the best visual quality and least amount of background noise. The SDME measure results show this improvement.

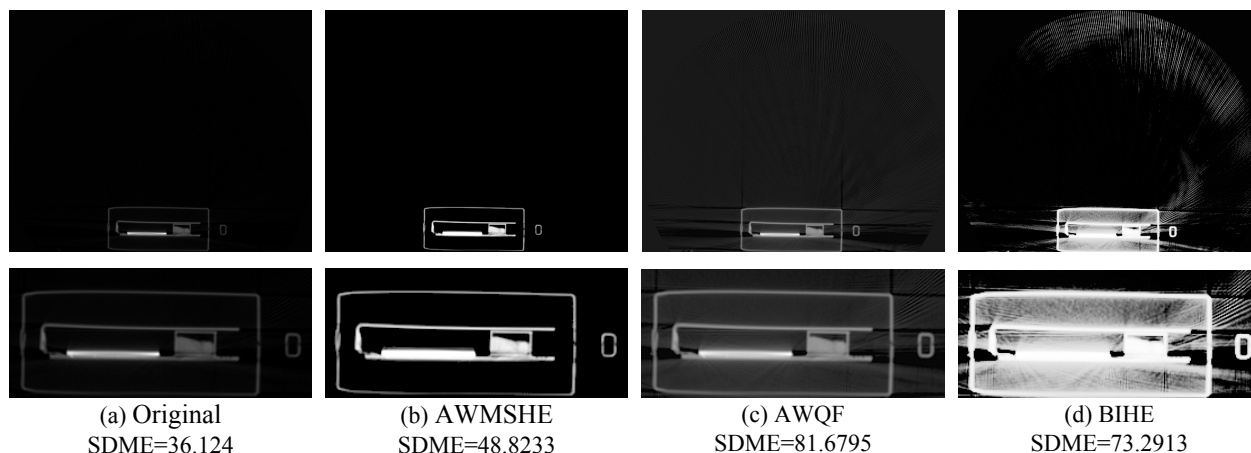| (a) Original | (b) AWMSHE | (c) AWQF | (d) BIHE |
| SDME=36.124 | SDME=48.8233 | SDME=81.6795 | SDME=73.2913 |

Fig. 15. Comparison of the image enhancement using different enhancement methods. The top row shows the original and enhanced images. The bottom row shows the cropped regions from the corresponding images above. (a) the original CT baggage image; (b) the image enhanced by AWMSHE; (c) the image enhanced by AWQF; (d) the image enhanced by BIHE. This demonstrates that the AWMSHE outperforms other methods.

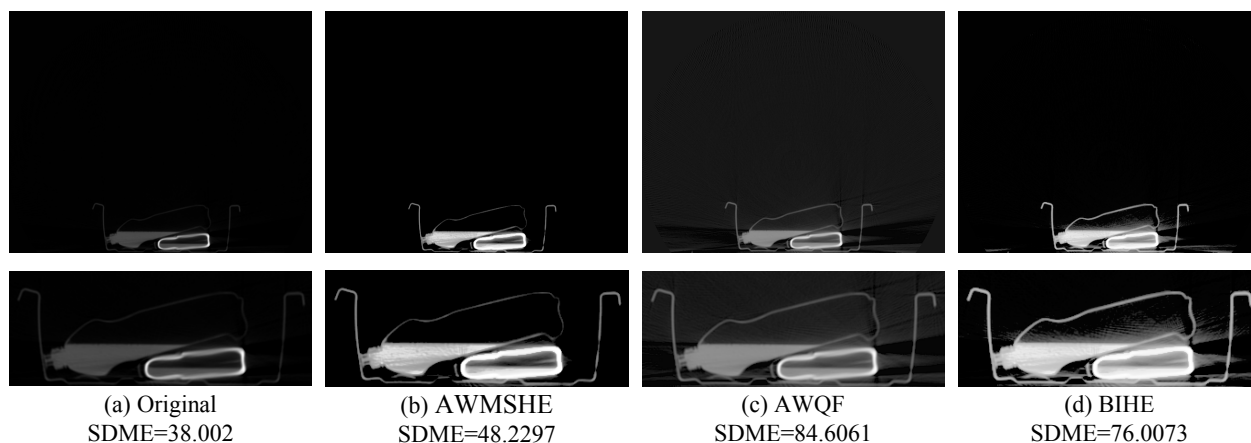| (a) Original | (b) AWMSHE | (c) AWQF | (d) BIHE |
| SDME=38.002 | SDME=48.2297 | SDME=84.6061 | SDME=76.0073 |

Fig. 16. Comparison of the image enhancement using different enhancement methods. The top row shows the original and enhanced images. The bottom row shows the cropped regions from the corresponding images above. (a) the original CT baggage image; (b) the image enhanced by AWMSHE; (c) the image enhanced by AWQF; (d) the image enhanced by BIHE. This demonstrates that the AWMSHE outperforms other methods.

7. CONCLUSION

In this paper, we have analyzed the characteristics of CT baggage images. The images contain background projection noise and have a low visual quality. To enhance the visual quality of these images while removing the background noise, we have introduced a new image enhancement algorithm which integrates alpha-weighted mean separation with histogram equalization techniques.

The new enhancement algorithm has been proven to have the capability of significantly improving the global contrast of the original CT images as well as the visual quality of the objects while reducing the background noises. The computer simulations and comparisons have demonstrated that the presented new algorithm outperforms other enhancement methods in enhancing the CT baggage images. The quantitative SDME measure results and the 3D visualization have further proven the excellent enhancement performance of the presented algorithm. The new algorithm has potential applications in object segmentation and recognition in homeland security and medical applications.

ACKNOWLEDGEMENT

REFERENCES

[1]   David A. Schafer, Christopher C. Ruth, and Carl R. Crawford, "Air calibration scan for computed tomography scanner with obstructing objects," USA: Analogic Corporation, Peabody, MA., 1999.

[2]   David A. Schafer, Simon George Harootian, and Sorin Marcovici, "Area detector array for computer tomography scanning system," USA: Analogic Corporation, Peabody, MA., 2000.

[3]   Joung-Youn Kim, Lee-Sup Kim, and Seung-Ho Hwang, "An advanced contrast enhancement using partially overlapped sub-block histogram equalization," *Circuits and Systems for Video Technology, IEEE Transactions on,* vol. 11, no. 4, pp. 475-484, 2001.

[4]   Soong-Der Chen and A. R. Ramli, "Minimum mean brightness error bi-histogram equalization in contrast enhancement," *Consumer Electronics, IEEE Transactions on,* vol. 49, no. 4, pp. 1310-1319, 2003.

[5]   Yeong-Taeg Kim, "Contrast enhancement using brightness preserving bi-histogram equalization," *Consumer Electronics, IEEE Transactions on,* vol. 43, no. 1, pp. 1-8, 1997.

[6]   Soong-Der Chen and A. R. Ramli, "Contrast enhancement using recursive mean-separate histogram equalization for scalable brightness preservation," *Consumer Electronics, IEEE Transactions on,* vol. 49, no. 4, pp. 1301-1309, 2003.

[7]   Yu Wang, Qian Chen, and Baeomin Zhang, "Image enhancement based on equal area dualistic sub-image histogram equalization method," *Consumer Electronics, IEEE Transactions on,* vol. 45, no. 1, pp. 68-75, 1999.

[8]   M. Kim and Min Chung, "Recursively separated and weighted histogram equalization for brightness preservation and contrast enhancement," *Consumer Electronics, IEEE Transactions on,* vol. 54, no. 3, pp. 1389-1397, 2008.

[9]   Yicong Zhou, K. Panetta, and S. Agaian, "Mammogram Enhancement Using Alpha Weighted Quadratic Filter," in *Engineering in Medicine and Biology Society, 2009. EMBC 2009. Annual International Conference of the IEEE*, Minneapolis, Minnesota, 2009, pp. 3681-3684.